Nuclear magnetic resonance study of the diffusion of bound and free fluorine interstitials in alkaline-earth fluorides doped with trivalent impurities*

Sherman H. N. Wei† and David C. Ailion
Department of Physics, University of Utah, Salt Lake City, Utah 84112
(Received 14 October 1977)

When alkaline-earth fluorides are doped with trivalent impurities, interstitial fluorines are created to maintain charge neutrality. We have performed NMR dipolar-energy relaxation measurements over a wide temperature range and have observed the diffusion of both free and locally bound fluorine interstitials $F_{(i)}^-$ in the extrinsic region. We have observed that these motions depend strongly on the host-crystal lattice parameter. In particular, we have observed that the motion of $F_{(i)}^-$ which is at the nearest neighbor (nn) site to the trivalent impurity dominates the relaxation above room temperature in $CaF_2:Y^{3+}$ but is unobserved in $BaF_2:Y^{3+}$. In addition, a second type of bound $F_{(i)}^-$ motion, characterized by a much smaller activation energy, appears over a very narrow temperature range (150–185°C) in $CaF_2:Y^{3+}$, but over a large temperature range (below room temperature to 130°C) in $BaF_2:Y^{3+}$. $SrF_2:Y^{3+}$ shows similar behavior over a temperature range (54–160°C), which is intermediate between that of $CaF_2:Y^{3+}$ and $BaF_2:Y^{3+}$. Possible explanations in terms of the motion of a more remotely bound $F_{(i)}^-$ [e.g., at a next-nearest-neighbor (nnn) site] and the motion of $F_{(i)}^-$ near clusters of dipoles are discussed. We measured activation energies for all these $F_{(i)}^-$ motions. A comparison of our results with those by other techniques (specifically, EPR, ENDOR, optical spectroscopy, ionic conductivity, ionic thermocurrent, dielectric and anelastic loss) is also given.

I. INTRODUCTION

In recent years, considerable interest has arisen in the determination of the microscopic nature of diffusive motions in ionic crystals. A number of different experimental techniques exist for studying the defects responsible for the motions as well as the motions themselves. The static techniques [e.g., electron paramagnetic resonance (EPR), optical absorption, electron-nuclear double resonance (ENDOR)] tend to provide information about the nature and site symmetry of the defects; whereas the dynamic techniques [ionic conductivity, ionic thermocurrent (ITC), dielectric relaxation, anelastic relaxation, radioactive tracers, and nuclear magnetic relaxation] tend to measure such properties as diffusion constant and activation energy. Many of these techniques, however, are limited in the kinds of information which they can provide (e.g., ITC measurements are restricted to bound defects).

Nuclear magnetic resonance (NMR) has many advantages over other techniques. It measures the bulk behavior of the paramagnetic nucleus which is studied and, accordingly, is not affected appreciably by such imperfections as grain boundaries and dislocations (which, for example, may dramatically affect the results of an ionic conductivity experiment. Furthermore, NMR can often detect diffusive and reorientational motions over a very wide temperature range, corresponding to a large range in jump frequencies. Accordingly, it has the capability of studying many different mechanisms which dominate the diffusion in different temperature regions. With the non-NMR techniques, one must often change techniques to study different diffusion mechanisms.

In the present experiment we studied, using NMR techniques, ^{19}F dipolar energy relaxation due to motions of fluorine interstitials in three alkaline-earth fluorides (CaF_2, SrF_2, and BaF_2) doped with different trivalent impurities (Y^{3+}, Sm^{3+}, Ce^{3+}, and La^{3+}).

The fluorite structure, shown in Fig. 1, consists of a simple cubic array of F^- ions with divalent cations (Ca^{2+}, Sr^{2+}, Ba^{2+}) occupying the body-center positions of every other cell. A trivalent impurity (M^{3+}) will substitute for a divalent cation and create a fluorine interstitial $F_{(i)}^-$ in a nearest-neighbor (nn) site (as shown in Fig. 1) or in a next-nearest-neighbor (nnn) site or possibly even further away.

NMR techniques are very suitable for studying this particular system since the only stable isotope of fluorine has a spin[1] of $\frac{1}{2}$ and therefore no quadrupole moment. Furthermore, the large γ value for ^{19}F provides us with good sensitivity for NMR detection. In addition, ^{19}F is the only abundant nucleus having a magnetic moment. Also, the cation Ca^{2+} is reported to be much less mobile[2] than the anion F^-.

NMR relaxation time measurements can provide information pertaining to the microscopic details of atomic motions. Measurements of the slopes of plots of relaxation times versus reciprocal temperature determine the activation energy for the diffusion process. Because of its greater sensitivity to infrequent motions,[3] it is

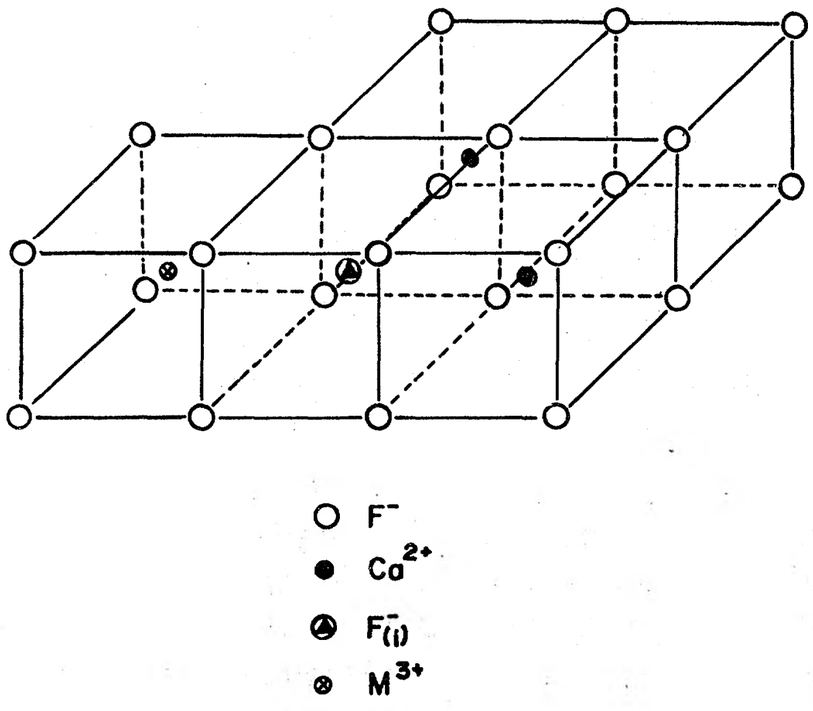

FIG. 1. Crystal structure of CaF_2, with one Ca^{2+} replaced by a trivalent impurity (M^{3+}) and charge compensated by a fluorine at a nearest-neighbor interstitial site.

often advantageous to measure the dipolar relaxation time T_{1D} rather than the spin-lattice relaxation time T_1.

In our experiments on $F^-_{(i)}$ diffusion in the fluorites, we can determine whether the dipolar relaxation in a particular temperature range is dominated by a single relaxation mechanism. It is possible to fit the ln T_{1D} versus $1/T$ curve by a straight line only in a temperature range dominated by a single mechanism. If many mechanisms are present and have different activation energies, each mechanism could in turn become the dominant mechanism over some temperature region. The observation of such different mechanisms requires the ability to see changes in the slope of the relaxation time versus reciprocal temperature. If one wishes to detect several mechanisms, it is then necessary to measure relaxation times over a very wide temperature range. Thus, a major advantage of measuring T_{1D}, which provides motional information over a wide temperature range, is that we may study, with the same experimental technique, many different diffusion processes simply by varying the temperature. In particular, as we shall see in Sec. III, we have studied the motions of both free and bound $F^-_{(i)}$ ions. Furthermore, we have been able to characterize to some extent the nature of the bound diffusion and have observed slopes for the diffusion of nn $F^-_{(i)}$ ions which are different from those for $F^-_{(i)}$ ions which are further away from a trivalent impurity.

In the present experiment, we were able to identify the dominant relaxation mechanisms by using the following kinds of information: (i) a comparison of our activation energies with those obtained by other research, (ii) a comparison between our data from doped and undoped samples, (iii) observations of the effect on the relaxation mechanism of varying the M^{3+} dopant concentration, and (iv) effects of varying the host lattice and dopant size.

II. EXPERIMENTAL CONSIDERATIONS

A. Sample

All the crystals used in this experiment were ordered from Optovac Company and were grown under high vacuum by the Stockbarger-Bridgman method.[4] Lead fluoride was used as a scavenger to reverse any prior hydrolysis reactions and to prevent any further reaction between water vapor and the pure fluoride. This procedure can effectively eliminate oxygen as an impurity.[5]

The dopant material was precision weighed and then introduced into the melt. Since the rare earths are highly soluble in the fluorites (accommodation coefficients are of order unity for Y^{3+} and Ce^{3+}), Optovac claims that the final dopant concentrations are within 1% of those reported in our samples.[5] The dopant is reported[5] to have a homogeneity throughout our samples of better than 5% for dopant concentrations less than 0.5 mole%. (The dopant homogeneity can be checked[5] by doping with "colored" impurities like Nd^{3+} and Pr^{3+}. Furthermore, we broke our CaF_2:0.035-mole%-Y^{3+} sample into two parts and observed identical relaxation time behavior for the two parts.) In order to minimize any effects due to a nonuniform distribution of dopant, we measured activation energies only for the less heavily doped samples (0.0035 mole% dopant in CaF_2 and SrF_2 and 0.01 mole% dopant in BaF_2). All our crystals are claimed[5] to have a purity of between 99.99 and 99.999 mole% before doping. So, unless the doping process introduces additional impurities along with the dopant, our background impurity level should be between 0.001 and 0.01 mole%. Spectrographic analyses on some of our samples, though possibly unreliable, are consistent with these figures. The most likely impurities are almost certainly trivalent ions, since they enter most easily and others hardly enter at all. Additional trivalent impurities would just shift our curves similar to the effects of additional dopant.

All the samples had cylindrical shape, 29/64-in. diam. and 1-in. length with the cylindrical axis parallel to a [100] direction. The other perpendicular [100] directions were determined by x-ray crystallography and then rechecked by comparing with the (111) cleavage plane.

B. Experimental procedure

The experimental procedure is mainly that of adiabatic demagnetization in the rotating frame[6]

(ADRF) applied to the ^{19}F spins. The dipolar relaxation time T_{1D} is determined by plotting the resulting magnetization as a function of time in the demagnetized state, according to the following relation:

$$M = M_0 \exp(-t/T_{1D}) \quad . \tag{1}$$

In all our data, M was plotted over at least two decades and was observed to be exponential within our indicated standard deviation. Similar to T_1 in the high-temperature region, a plot of T_{1D} versus $1/T$ gives rise to a minimum[3] when $\tau \sim \omega_d^{-1} \sim T_2$. At the low-temperature side of this minimum, the so-called "strong-collision theory"[7] applies and can be used to show that $T_{1D} \propto \tau$. On the high-temperature side of the minimum, T_{1D} is inversely proportional to τ.

If the atomic jump time τ satisfies an Arrhenius equation, $\tau = \tau_0 \exp(E/kT)$, the slope on the low-temperature side can be used to determine the activation energy.

C. Apparatus

The spectrometer used in this experiment can be divided into four major parts—rf transmitter system, signal receiving system, temperature control system, and computer control system. The circuitries of the first three parts are adopted from those used by Ho.[8] The major modification made here is a computer control system which produces a sequence of ADRF pulses whose demagnetization durations can be typed in externally from a Teleray keyboard. Furthermore, it collects the NMR free-induction decay signals corresponding to a particular demagnetization duration, stores them on the memory disk, and averages them. The apparatus, especially the computer control system, is described in more detail elsewhere.[9]

III. EXPERIMENTAL RESULTS

The primary purpose of the present experiment is to study the dipolar relaxation due to fluoride-ion motion in doped fluorites. In this study, we measured the temperature dependence of the dipolar relaxation time T_{1D} as a function of three different parameters which were varied: the host lattice, the concentration of dopant, and the ionic radius of the dopant. In particular, our measurements were performed on CaF_2, SrF_2, and BaF_2 whose lattice parameters[10] are 5.46, 5.81, and 6.21 Å, respectively. These samples were doped with a number of different trivalent impurities of different ionic radii[11]: Y^{3+} (0.93 Å), Sm^{3+} (1.04 Å), Ce^{3+} (1.11 Å), and La^{3+} (1.15 Å). Furthermore, in all three fluorites, we used dopant concentrations of Y^{3+} of 0, 0.0035, 0.01, 0.035, 0.1, and 0.35 mole%.

A. CaF_2:Y^{3+}

Figure 2 shows a semilog plot of the dependence of T_{1D} on inverse temperature for different Y^{3+} dopant concentrations. We can divide each curve into four different temperature regions which will be discussed individually.

1. Region IV

In this temperature region $[(3.4–2.9) \times 10^{-3}\ K^{-1}]$, the relaxation curves show two phenomena. First, the slopes of the data curves are different from one another, decreasing with increasing Y^{3+} concentration. Second, the relaxation time at any given temperature decreases with increasing Y^{3+} dopant concentration.

The first phenomenon indicates that there may exist a second source of relaxation in this region which becomes increasingly competitive in the higher Y^{3+} doped samples. The most likely candidate for this mechanism could be the relaxation mechanism which dominates the relaxation pro-

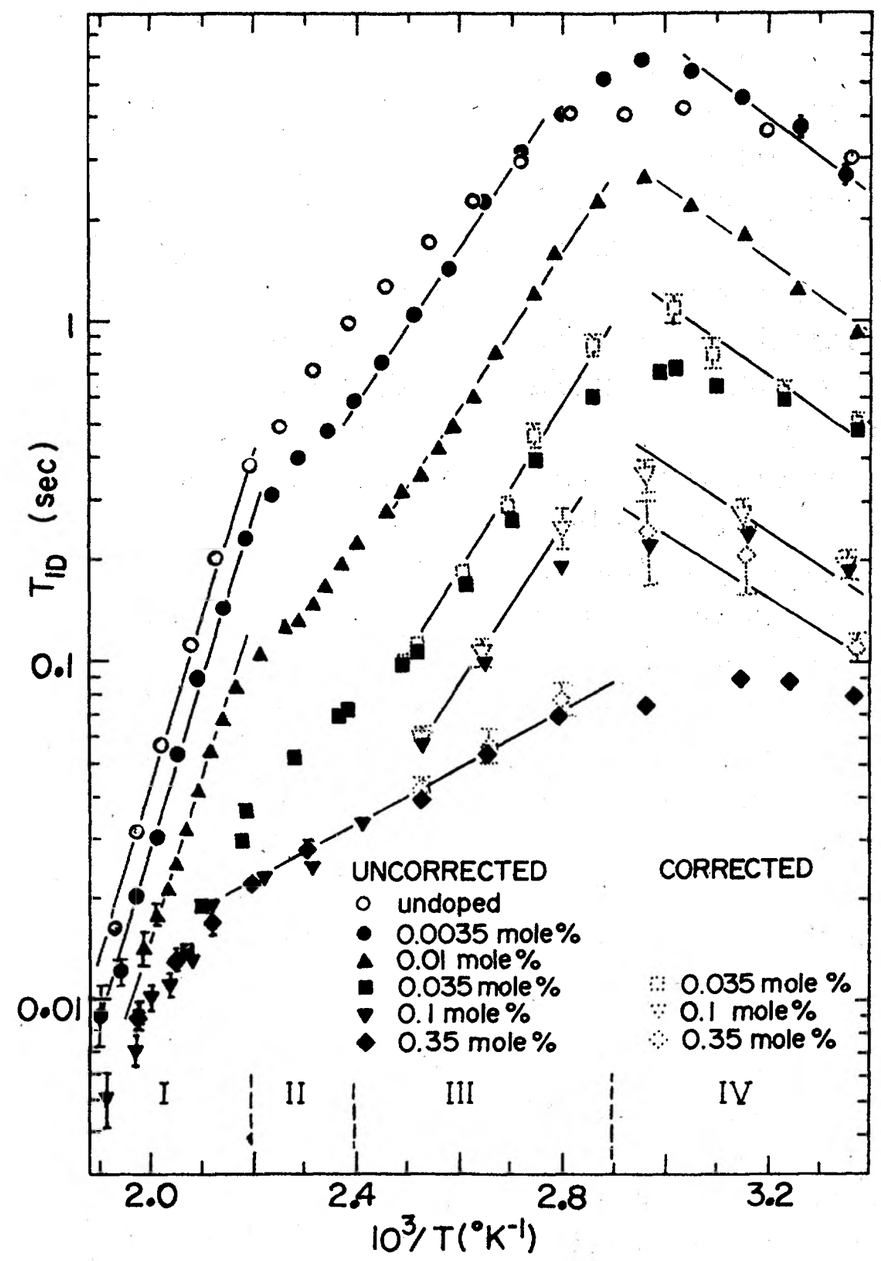

FIG. 2. Relaxation time vs reciprocal temperature in CaF_2 doped with different Y^{3+} concentrations. Solid lines represent least-square fits to the data.

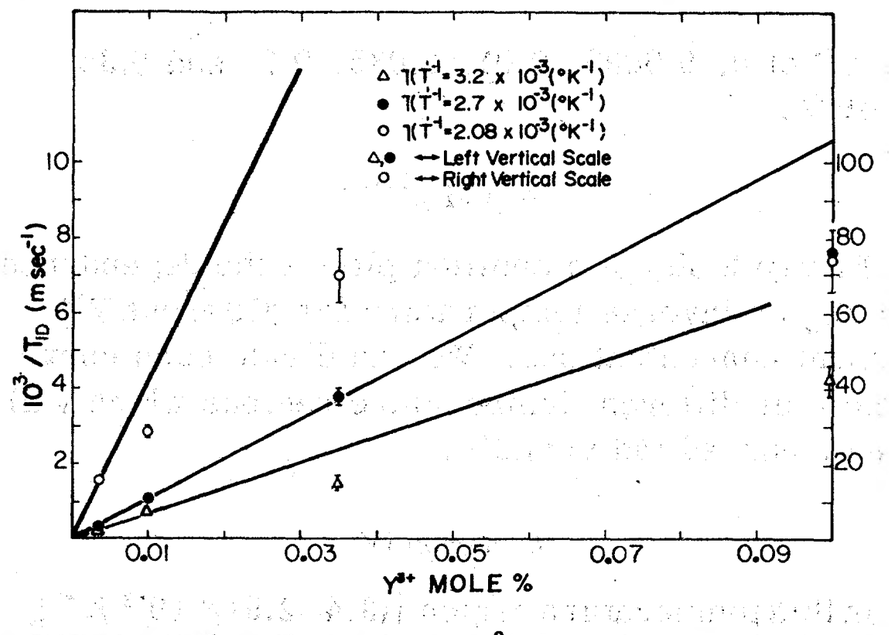

FIG. 3. Relaxation rate vs Y^{3+} dopant concentration in CaF_2 at three different temperatures.

cess in region III [$(2.9-2.4)\times10^{-3}$ K^{-1}]. By extrapolating the data curve from region III into region IV and then subtracting off the contribution due to region III using the following equation,

$$\frac{1}{(T_{1D})_{IV}}=\frac{1}{(T_{1D})_{data}}-\frac{1}{(T_{1D})_{III}}\ , \qquad (2)$$

we found that all the corrected data curves (the solid lines in Fig. 2) for $(T_{1D})_{IV}$ are indeed parallel to each other and have an activation energy of 0.23 ± 0.03 eV. (The indicated error represents the standard deviation of our data and does not include any estimate of the error due to the correction process.)

The triangles in Fig. 3 show the dependence of the corrected relaxation time $(T_{1D})_{IV}$ on the Y^{3+} dopant concentration. The data indicate that the relaxation increases initially in proportion to the Y^{3+} dopant concentration and then gradually saturates.

We do not thoroughly understand the source of the corrected relaxation in this region. One possibility is that it arises from a paramagnetic impurity which is introduced with the YF_3 dopant powder and would thus be proportional to the Y^{3+} concentration. A second possibility is that the relaxation is due to $F^-_{(i)}$ which are introduced by the Y^{3+} to maintain charge neutrality but which have a different jump mechanism than the $F^-_{(i)}$ which are responsible for the relaxation in regions III, II, and I. These possibilities will be discussed in more detail later.

2. *Region III*

This region extends over the range of inverse temperatures $(2.9-2.4)\times10^{-3}$ K^{-1}. Except for the undoped and most heavily doped (0.35 mole% Y^{3+}) samples, the curves have approximately the same slope, slightly decreasing with increasing dopant concentration. The observed slope in region III is slightly lower than would be the case were there no contribution from the mechanism of region IV, as we discussed above. Nevertheless, by extrapolating the corrected data curves from region IV into region III, we can also correct the data in region III. Like in region IV, the corrected data curves in region III are also parallel to each other as is shown in Fig. 2, thereby indicating that all the curves in this region probably arise from the same mechanism. We measured the activation energy to be 0.45 ± 0.02 eV. The corrected relaxation rate in this region is proportional to the Y^{3+} dopant concentration up to 0.035 mole% as is shown by the solid circles in Fig. 3, thus suggesting that the dominant relaxation mechanism in this temperature region probably arises from $F^-_{(i)}$ due to the Y^{3+} impurities.

From EPR,[12-15] ENDOR,[16-18] and optical spectroscopy[14,15,19-25] experiments, it is well established that the major charge-compensating F^- ions in CaF_2:M^{3+} are those located in interstitial sites which are nearest neighbor (nn) to the trivalent dopant impurities in the low dopant concentration samples. For the more heavily doped samples, the effective number of free M^{3+}-$F^-_{(i)}$ pairs decreases and eventually disappears due to clustering between the M^{3+}-$F^-_{(i)}$ dipolar pairs.[19,20,25-30]

ITC, dielectric loss, and anelastic relaxation measurements have been used to study relaxation processes of the trivalent impurity—nn $F^-_{(i)}$ dipolar complex. Their measured activation energy is about 0.4 eV, as shown in Table I, which compares favorably to our measured value of 0.45 ±0.02 eV in this region.

An interesting feature of our data is the abrupt termination of region III at around 150 °C which implies, as we shall see, the termination of this particular relaxation mechanism. Furthermore, Rewaj[30] and Franklin and Marzullo[27] all observed that the dominant tetragonal EPR spectral line of Gd^{3+} in CaF_2:Gd^{3+} disappears at about the same temperature (150 °C). This phenomenon will be discussed in more detail when we discuss region II.

The fact that all of these results and observations are consistent with our data suggests that the $F^-_{(i)}$ ions which dominate the NMR relaxation in region III are those located in the interstitial position which is nn to Y^{3+}. Further evidence for this interpretation arises from the way the NMR relaxation in the region varies with lattice distance as we go to SrF_2:Y^{3+} and BaF_2:Y^{3+} and will be described in a later section.

3. *Region II*

In this temperature region [$(2.4-2.2)\times10^{-3}$ K^{-1}], the slopes of the data curves are smaller than

TABLE I. Activation energies of local bound fluorine interstitials.

Crystal	Dopant	Technique	Activation energy (eV)	Defect jump time (sec)	Remark	Reference
CaF_2	Y^{3+}(0.01 mole%)	Dielectric loss	1.16 ±0.08	3×10^{-14}		31
	Y^{3+}	Anelastic loss	1.2	10^{-15}		32
	Sm^{3+}	NMR T_1 measurement	0.36 and 0.53	10^{-14}	Former one is for undoped samples. The other one is for doped sample.	33
	Ce^{3+}(0.01–0.05 mole%)	ITC	0.46±0.02 to 0.36	$(6 \pm 4) \times 10^{-15}$	E_a depends on the number of free dipoles.	34
	Gd^{3+}	ESR line broadening and dielectric loss	0.38	8.2×10^{-14}		35
	Y^{3+}(0.0035–0.1 mole%)	NMR T_{1D} measurement	0.45 ±0.02 eV			a
	Gd^{3+}	ITC	0.39 ±0.01 and 0.167±0.005	1.2×10^{-13} and 2×10^{-13}	Two relaxation peaks were observed.	36
	Er^{3+}	ITC	0.386±0.008 and 0.147±0.004	2×10^{-13} and 3×10^{-13}	Two relaxation peaks were observed.	36
	From Ce^{3+} to Yb^{3+}	ITC	0.51 to 0.56	6×10^{-17} for Ce^{3+} to 4×10^{-18} for Yb^{3+}	E_a is independent of dopant size.	37
	Gd^{3+}(0.00–0.45 mole%)	ITC	0.54 – 0.47	1.01×10^{-14} to 8×10^{-17}	E_a is maximum for 0.08 mole % CaF_2:Gd^{3+}	37
	Ce^{3+}, Pr^{3+}, Sm^{3+}, Eu^{3+}, and Tb^{3+}	ITC	0.36 to 0.47	10^{-12} to 10^{-14}	E_a increases with dopant size.	38
	Gd^{3+}(0.1 mole%)	ITC	0.42 and 0.69		Two relaxation peaks were observed.	39
	Se^{3+}, Yb^{3+}, Tm^{3+}, Er^{3+} Y^{3+}, Dy^{3+}, Gd^{3+}, Eu^{3+}, Nd^{3+}, Ce^{3+}, U^{3+}	ITC	0.38 to 0.42	2×10^{-14} to 2×10^{-15}	E_a increases with dopant size.	40
	Ce^{3+}(0.01 mole%)	Dielectric loss	0.46 ±0.01	5 ± 10^{-13}		41
	Er^{3+}(0.001–3.0 mole%)	Dielectric loss	0.028, 0.15, 0.4, 0.5, and 0.7		Five relaxation peaks were observed.	42
	Gd^{3+}(0.01–0.27 mole%)	Dielectric loss and anelastic loss	0.42, 0.16, 0.2, and 1.1 – 1.2		Four relaxation peaks were observed.	43

TABLE I. (*Continued*)

Crystal	Dopant	Technique	Activation energy (eV)	Defect jump time (sec)	Remark	Reference
SrF_2	Y^{3+}(0.01 mole %)	Dielectric loss	1.01 ±0.02			31
	Gd^{3+}(0.1 mole %)	ITC	0.45 and 0.62	10^{-14} and 4×10^{-14}	Two relaxation peaks were observed.	39
	Y^{3+}(0.0035–0.35 mole %)	NMR T_{1D} measurement	0.46 ±0.03 0.17 ±0.03		Two relaxation regions were observed.	a
	Eu^{3+}	ITC	0.26, 0.28, and 0.33	2×10^{-9}, 5×10^{-8}, 2×10^{-9}	Three relaxation peaks were observed.	38
BaF_2	Gd^{3+}	ITC	0.46 and 0.60	10^{-12} and 10^{-14}	Two relaxation peaks were observed.	39
	Y^{3+}(0.01 mole %)	Dielectric loss	0.86 ±0.02			31
	Y^{3+}(0.01–0.1 mole %)	NMR T_{1D} measurement	0.10 ±0.03			a

[a]Results of present experiment.

those in the lower-temperature region III. It is impossible to explain this behavior simply by postulating that an extra relaxation mechanism becomes important in region II in addition to that which dominates region III. Since the observed relaxation rate would be the sum of all component rates, the observed relaxation time would have to be smaller than any component time. As a result, the higher activation energy process would have to dominate at higher temperatures (as in region II) and the lower activation energy process would dominate at lower temperature (region III), in contrast to our observations.

We are forced to come to one of the following possible conclusions. Either the decrease in slope is an NMR artifact (like the onset of a relaxation time minimum) and not a true decrease in activation energy, or it implies that the process responsible for the relaxation in region III changes in region II (as in the case of a phase transition). Explanations of both kinds were given in the past. For example, Ho and Ailion[8] attributed region II in CaF_2:Y^{3+} to be a shallow T_{1D} minimum region due to the region-III relaxation mechanism. Such a minimum would occur when the jumping rate of the local $F^-_{(i)}$ ions approaches approximately $\omega_d \sim 1/T_2$ (10 KHz in this case). Rewaj[30] measured the EPR spectra of CaF_2:Gd^{3+} and observed that the tetragonal spectrum of Gd^{3+} with $F^-_{(i)}$ in its nn interstitial site completely disappears before the temperature reaches 200 °C, which he attributed to the dissociation of nn $F^-_{(i)}$ from the nearby Gd^{3+}. Franklin and Marzullo[27] repeated the experiment and confirmed this phenomenon by finding that the tetragonal spectrum of Gd^{3+} disappears around 150 °C. They attempted to explain this behavior by considering the possibility that the nn $F^-_{(i)}$ ions become nonlocal at temperatures above 150 °C. In order to test this possibility, they compared the results of a sample which was very slowly cooled with results of a sample which was rapidly quenched from temperatures above 150 °C to liquid-nitrogen temperatures. If nn $F^-_{(i)}$ ions became nonlocal at temperatures greater than 150 °C, one would expect a reduction in intensity of the tetragonal signal obtained in the rapidly quenched sample as compared to the slowly cooled sample. However, they observed no difference in signal intensity for these two cases and were thus led to the conclusion that the $F^-_{(i)}$ are localized in both regions. They tried to explain their disappearance of signal as due to broadening[44] which would occur when the jump time is comparable to the microwave frequency (9 GHz). A difficulty with their interpretation is that it would predict the temperature of the transition to be very different at our radio frequencies than at their microwave fre-

quency, in striking contrast to our observation that the region II–region III transition occurs at about 150 °C.

We are not certain of the cause of the low-activation-energy behavior in region II. Nevertheless, both the disappearance of the tetragonal spectrum and the onset of the low activation energy motion above 150 °C appear to be consistent with several possible explanations. One possibility is that region II is characterized by partial, but not complete, dissociation of the $F^-_{(i)}$ ions from their M^{3+} impurities. The lower activation energy could occur if the barrier separating equivalent distance $F^-_{(i)}$ sites is lower than that separating nn $F^-_{(i)}$ sites. A second possibility is that region II is characterized by the formation of complexes of M^{3+}-$F^-_{(i)}$ dipoles which no longer have tetragonal symmetry. The lower activation energy would occur if the barrier hindering the motions of the $F^-_{(i)}$ near the complex is less than that between equivalent nn sites of a single M^{3+} ion. Both of these explanations will be discussed in more detail shortly.

Complete dissociation of nn $F^-_{(i)}$ into remote cubic sites can be ruled out as a possible explanation for the disappearance of the tetragonal spectrum, since complete dissociation not only would have given Franklin and Marzullo[27] a better chance to freeze the dissociated $F^-_{(i)}$ in the nonlocal cubic sites by fast quenching but would have caused the number of nonlocal $F^-_{(i)}$ to show a corresponding increase in the highest-temperature region (region I). Neither of these effects were observed. This last point will be discussed further when we later talk about region I. We did similar experiments and compared T_{1D} of a normally grown, slowly cooled CaF_2:Y^{3+} with that of a fast-quenched CaF_2:Y^{3+}. Our result is seen in Fig. 4 which shows clearly that the relaxation rate due to nonlocal $F^-_{(i)}$ (in region I) is *not* increased for the quenched sample. Rather, we observe an overall decrease of $F^-_{(i)}$ both local and nonlocal (i.e., an increase in T_{1D}) in all sites, with nonlocal $F^-_{(i)}$ affected more than nn $F^-_{(i)}$. (Even though this overall increase in T_{1D} is reasonable, we have no explanation for the greater increase of T_{1D} in region I than in the other regions. Attempts by other research groups[30,45] to suppress the axial components of the EPR spectrum by annealing and quenching have not been consistently successful either.)

Similar phenomena[46] also occur in AgBr:Cd^{2+}, in which the ^{79}Br NMR line was observed to broaden with decreasing intensity above 200 °K. This behavior was attributed to the onset of the dissociation of the Cd^{2+}:$Br^-_{(i)}$ pair.

Other workers, using dielectric loss methods,

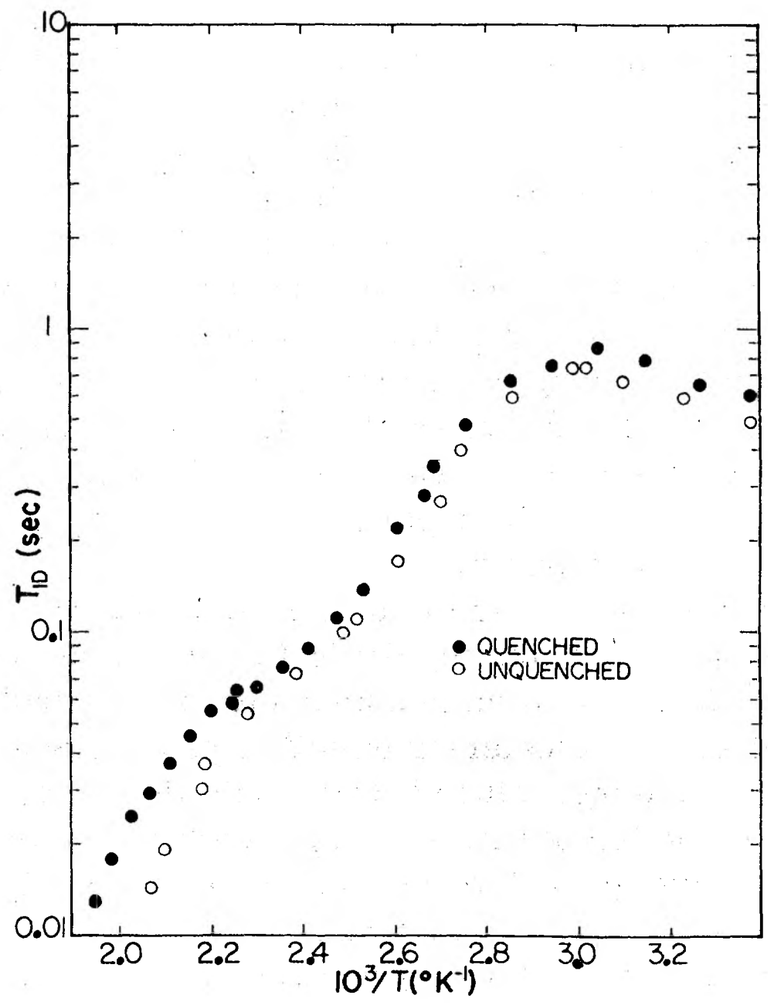

FIG. 4. Comparison of relaxation curves between thermally quenched and unquenched CaF_2:0.035 mole % Y^{3+}.

have observed similar low activation energy phenomena[47,48] at lower temperatures in rare-earth-doped calcium fluoride. In particular Edgar and Welsh[48] *tentatively* assigned their phenomena to aggregation effects (i.e., clusters of defects). It is tempting to speculate that our low activation energy data may also be due to the motion of $F^-_{(i)}$ ions near clusters of defects. This explanation is in agreement with the following observations:

(a) The relaxation rate in region III is not strictly proportional to Y^{3+} dopant concentration, but levels off at higher (e.g., 0.1 mole%) Y^{3+} concentrations until, at 0.35 mole% Y^{3+}, region III is no longer discernable (see Fig. 2). The fact that our high concentration slope in region III, which is due to motion near clusters, is comparable to the slope of region II suggests that the data in region II also arises from motion near clusters.

(b) The EPR line due to centers having tetragonal symmetry disappears at approximately the same temperature as that at which we observed the change in slope of the NMR relaxation curves. Since the site symmetry of a cluster will in general not be tetragonal, it is reasonable to expect that the formation of clusters will be associated with a decrease in the intensity of the tetragonal EPR spectra.

(c) A careful inspection of Fig. 2 indicates that the boundary between regions II and III shifts to lower temperatures for more heavily doped samples. This behavior can be explained by the

cluster model in that more heavily doped samples will contain many more clusters. Thus, in these samples, clusters will dominate the relaxation over a wider temperature range.

A feature of our data which should be noted is that region-II type behavior appears in our measurements over much wider temperature ranges in samples having larger lattice parameters (e.g., SrF_2 and BaF_2, as we shall see). It is not obvious that clusters should form more easily in samples having a larger lattice parameter, like BaF_2, as this data would imply.

Unfortunately, there is a more serious major problem with explaining the NMR relaxation in our region II as due to motion near clusters. First, why does the "clustering effect" appear as one *raises* the temperature? One would think that raising the temperature would oppose the formation of clusters and would in fact cause already existing clusters to break apart, rather than the opposite.[27,30] Furthermore, even though Edgar and Welsh[48] observed at low temperatures dielectric relaxations in CaF_2:Gd^{3+} also having low activation energies (0.15 and 0.076 eV), they observed no evidence of clusters in room-temperature EPR spectra.

Because of the above difficulties in explaining our region II as due to $F^-_{(i)}$ motion near clusters, we suggest an alternative possibility for explaining our data. This possibility is that, above 150 °C, most nn $F^-_{(i)}$ may suffer a fairly sudden "partial dissociation"; that is, they may jump to a more remote but still bound site relative to the M^{3+}. An example of this process would be for the dominant jumping mechanism of nn $F^-_{(i)}$ to be no longer nn→ nn reorientation but rather a motion in which the distance between M^{3+} impurity and nn $F^-_{(i)}$ constantly varies (e.g., nn→ nnn motion and vice versa as suggested by Catlow[49]). Alternatively, the motion could be between equivalent nnn sites. This partial or incomplete dissociation would explain the difficulty or inefficiency in the quenching process, the observed line-broadening effect, the disappearance of the tetragonal EPR spectra, and the change in slope of the NMR relaxation curve, as described before. Furthermore, the dominance of this low activation energy behavior increases with lattice parameter as we go from CaF_2 to SrF_2 to BaF_2 and appears to be correlated with increased intensity of trigonal (nnn) EPR spectra in SrF_2 and BaF_2. This point will be discussed further in Secs. III B and C of this paper. (It had been suggested[39] earlier that nnn complexes in CaF_2 reorient with an activation energy of around 0.7 eV, which would contradict the above suggestion that such motions have a much smaller activation energy. However, more recent work[47,48] has resulted in considerable evidence against this assignment of the 0.7 eV relaxation to nnn motions.)

The simple model of dividing $F^-_{(i)}$ in CaF_2 into two different species (i.e. local bound nn $F^-_{(i)}$ and nonlocal free $F^-_{(i)}$) is certainly inadequate to explain many other phenomena. Even though spectroscopy experiments indicate the dominance of the tetragonal, and to a lesser extent, cubic sites of $F^-_{(i)}$ in CaF_2, $F^-_{(i)}$ in other sites do exist and can also affect the experimental results. $F^-_{(i)}$ ions in these other sites are manifested not only in the supernumerous spectral lines in EPR and in optical spectroscopy but also in the various different spectral peaks detected by the ITC, dielectric, and anelastic relaxation measurements referred to earlier.

4. Region I

This region extends over the range of inverse temperature $(2.2-1.9)\times10^{-3}$ K^{-1}. For the undoped and two lightly doped samples, the slopes are the same, corresponding to an activation energy of about 1.04 ± 0.05 eV, which is the same as that obtained by ionic conductivity, NMR T_1, thermal annealing, and radioactive tracer techniques in the extrinsic region. Nonlocal free $F^-_{(i)}$ is believed to diffuse through the crystal by an interstitialcy jump mechanism.[50–52] The results of all these experiments are given in Table II.

From the data, we see that there are substantial numbers of nonlocal $F^-_{(i)}$ in the undoped sample, due probably to residual trivalent impurities. As the Y^{3+} dopant concentration increases, the number of nonlocal $F^-_{(i)}$ increases proportionately. The NMR relaxation rate soon saturates, however, at medium Y^{3+} concentration (i.e., 0.035 mole% Y^{3+}) as shown by the open circles in Fig. 3. The reason for this is that at the higher dopant concentration the number of nonlocal sites (i.e., far from the impurities) available for fluoride interstitials begins to decrease appreciably, since the number near the impurities becomes a large fraction of the total. Thus, even though the number of $F^-_{(i)}$ increases with Y^{3+} concentration, their effectiveness in contributing to nonlocal relaxation is reduced appreciably. However, this decrease in nonlocal F^- interstitial sites does not limit relaxation due to localized $F^-_{(i)}$ which saturates only at the even higher dopant concentrations at which clustering becomes important. Both of these effects are shown in Fig. 3. Osiko[63] did theoretical calculations of the $F^-_{(i)}$ site distribution as a function of M^{3+} dopant concentration in CaF_2 and his resulting distributions are consistent with our data in Fig. 3.

Due to the great distance of nonlocal $F^-_{(i)}$ from

TABLE II. Activation energy for motion of extrinsic free fluorine interstitials.

Crystal	Activation energy (eV)	Technique	Reference
CaF_2	1.1–1.2	Ionic conductivity	2
	1.02	Ionic conductivity	53
	1	Ionic conductivity	54
	1.0	Thermal annealing	55
	0.9	Radioactive tracer	56
	1.5	Charge reduction	57
	1.56	Ionic conductivity	58
	1.04 ± 0.05	NMR T_{1D} measurement	a
SrF_2	0.94	Ionic conductivity	53
	1.01	Ionic conductivity	59
	0.7–0.76	NMR T_1 measurement	60
	0.88 ± 0.01	NMR T_{1D} measurement	a
BaF_2	0.62	NMR T_1 measurement	61
	0.79	Ionic conductivity	62
	0.82 ± 0.03	NMR T_{1D} measurement	a

[a]Results of present experiment.

Y^{3+} impurities, it is believed that the influence of the clustering effect is much less on them. For instance, Makovsky[19] found, in an optical spectroscopy study of rare-earth-doped calcium fluoride, $CaF_2:R^{3+}$, that spectral lines for an impurity cluster can be detected at about 0.01 mole%, and the tetragonal spectrum begins to weaken at about 0.1 mole%, vanishing entirely at about 2 mole%. The cubic site spectrum, however, is still observed at this high dopant concentration. The claim by Fenn *et al.*,[25] that there should be no more cubic EPR spectrum above 0.02 mole% dopant concentration, appears to be in error.

Evidence of the existence of unbound $F^-_{(i)}$ in undoped samples abounds also in the literature. For example, Merz and Pershan[28] observed that the undoped CaF_2, after x-ray irradiation, has thermoluminescence peaks similar to those of rare-earth-doped CaF_2. The fact that impurities in isolated cubic sites can be charge reduced by x-ray irradiation therefore verifies the existence of nonlocal $F^-_{(i)}$. Johnson *et al.*[64] also found a contribution to the dielectric loss in undoped CaF_2 from ohmic conduction of unbound $F^-_{(i)}$.

The decrease of the slopes for higher Y^{3+} doped samples is caused by the competitive relaxation contribution from region II, which increases for increasing Y^{3+} concentration since the nonlocal $F^-_{(i)}$ does not increase as fast as local bound $F^-_{(i)}$.

Ho and Ailion[8] reported similar behavior in rare-earth-doped CaF_2. They interpreted the slope of the relaxation time in region I to be proportional to $\phi_{\rm imp}+E_{M\,\rm I}$, where $\phi_{\rm imp}$ is the binding energy of the complex consisting of a trivalent impurity and nearest-neighbor $F^-_{(i)}$ and $E_{M\,\rm I}$ is the energy of motion of the nonlocal fluorine. The slope in region III would be proportional to $E_{M\,\rm III}$, the energy of motion for nn→nn jumps. Thus the difference in slopes is a measure of the binding energy plus the difference in barrier heights. Furthermore, they performed measurements of the anisotropy of T_{1D} in regions I, II, and III and measured in region I an anisotropy which agrees with calculations based on the strong-collision theory for nonlocal $F^-_{(i)}$ interstitialcy diffusion. They observed this anisotropy to disappear in regions II and III, as might be expected for the weak-collison situation in which only bound defects move.

B. $SrF_2:Y^{3+}$

SrF_2 with a lattice constant intermediate between that of CaF_2 and that of BaF_2 would be expected to exhibit behavior which is intermediate between that of the other two crystals. This indeed shows up in our data, as we shall see. Figure 5 shows the temperature dependence of the relaxation time T_{1D} for different Y^{3+} dopant concentrations. As before we divide each curve into different temperature regions and discuss them individually.

1. Region III

In this region $[(3.4–3.0)\times10^{-3}\ K^{-1}]$ undoped SrF_2 still resembles region IV of CaF_2. However, for all Y^{3+} doped samples, this region behaves more like region III in $CaF_2:Y^{3+}$, except that the slope of the corrected data is no longer the same for different samples, but gradually increases with Y^{3+} concentration and achieves the largest value of 0.46 ± 0.03 eV for the most heavily doped sample, $SrF_2:Y^{3+}$ (0.35 mole%), which we studied.

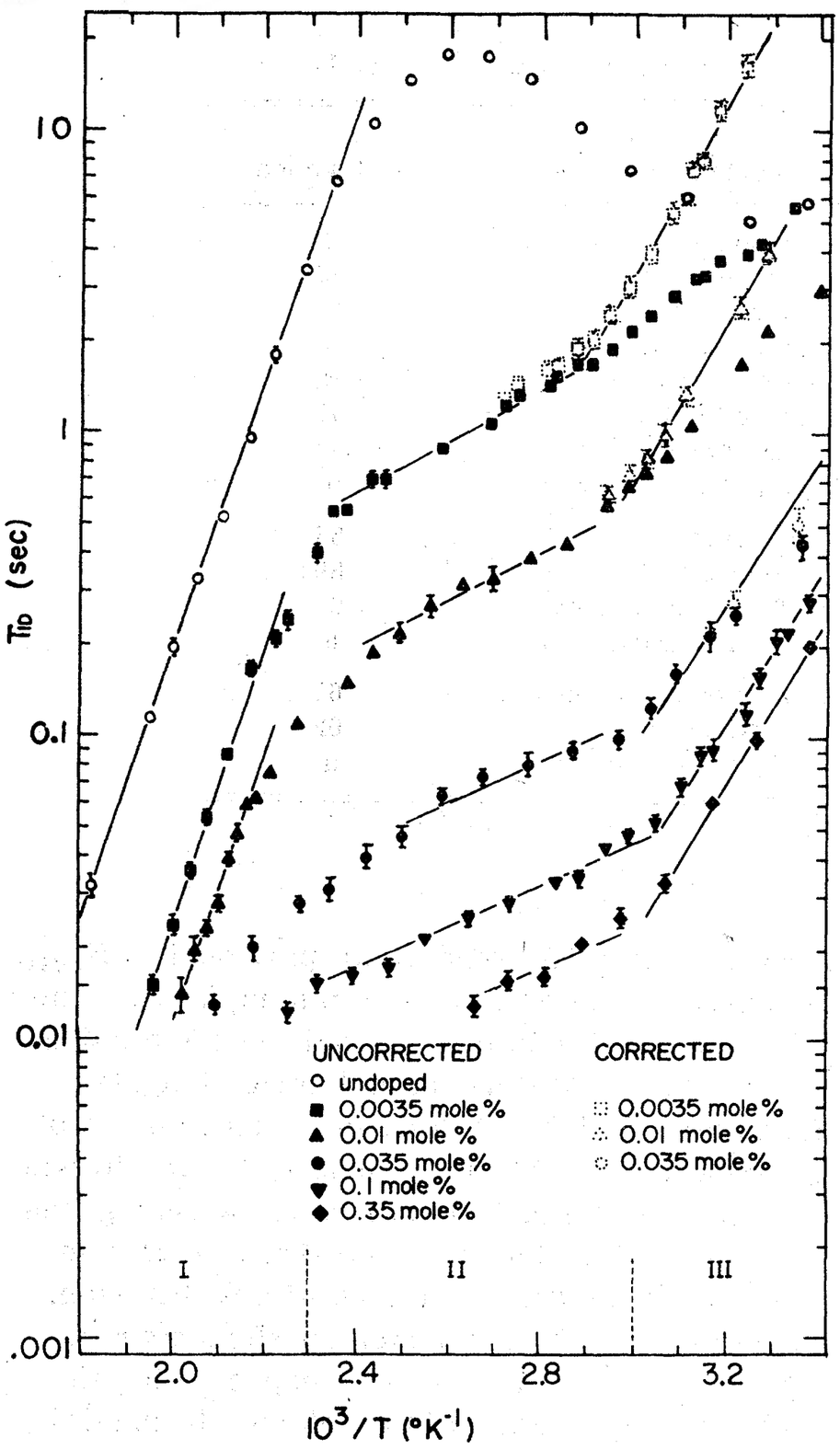

FIG. 5. Relaxation time vs reciprocal temperature in SrF_2 doped with different Y^{3+} concentrations. Solid lines in regions I and II are least-square fits to the data. Solid lines in region III are parallel to least-square fits to the 0.1- and 0.35-mole % data.

As we discussed for $CaF_2:Y^{3+}$, it is likely that the slope variation in this region is probably due to the existence of an additional contribution to the relaxation which contributes to the most lightly doped samples the most. If we hypothesize that the mechanism responsible for the low-temperature relaxation behavior of the undoped sample arises from impurities which are common to all the SrF_2 samples, doped and undoped, we should subtract its contribution (i.e., the relaxation rate measured for the undoped sample) from the observed relaxation curves of the doped samples in region III. If we do so, we indeed find that the corrected curves are now parallel, as shown in Fig. 5, which verifies the validity of our treatment. The solid lines in region III are all drawn assuming an activation energy of 0.46 ± 0.03 eV, which is the result of least-square fits to only the two most heavily doped samples, $SrF_2:Y^{3+}$ (0.35 mole %) and $SrF_2:Y^{3+}$ (0.01 mole %). It is clear that these corrected data points for our more lightly doped samples fit very well on the 0.46-eV activation energy lines. Region III of our SrF_2 samples now resembles region III of our CaF_2 samples and is probably due to the same mechanism, nn $F^-_{(i)}$ ions. (It was not important to subtract off the analogous contribution from the undoped sample in CaF_2, since its contribution to the relaxation rate was negligible at all temperatures.) Note that our data for SrF_2 exhibits no behavior in this temperature range like that of region IV of CaF_2.

Tetragonal lines of high intensity of R^{3+} in $SrF_2:R^{3+}$ have been observed by EPR[10,26,65,66] and optical spectroscopy.[19,67] Furthermore, a trigonal spectrum, which was barely observable in $CaF_2:R^{3+}$, has comparable intensity[10,19,26,65-69] in $SrF_2:R^{3+}$ to the tetragonal spectra. Those observations suggest that the probability of $F^-_{(i)}$ ions occupying nnn sites (which have trigonal symmetry) is higher in SrF_2 than in CaF_2.

The activation energy for reorientation of the M^{3+}–nn $F^-_{(i)}$ dipole has been measured by Kitts, Ikeya, and Crawford[39] for $SrF_2:Gd^{3+}$ and found to be 0.45 eV, which is indeed similar to that of our measurements in this temperature region. A list of all the results is given in Table I.

The curve of the corrected relaxation rate in region III versus Y^{3+} concentration is shown in Fig. 6. It indicates that the relaxation rate is proportional to the Y^{3+} dopant concentration up to 0.1 mole %, which is higher than for the case of $CaF_2:Y^{3+}$. This behavior might be due to a smaller clustering effect in SrF_2 since the larger lattice

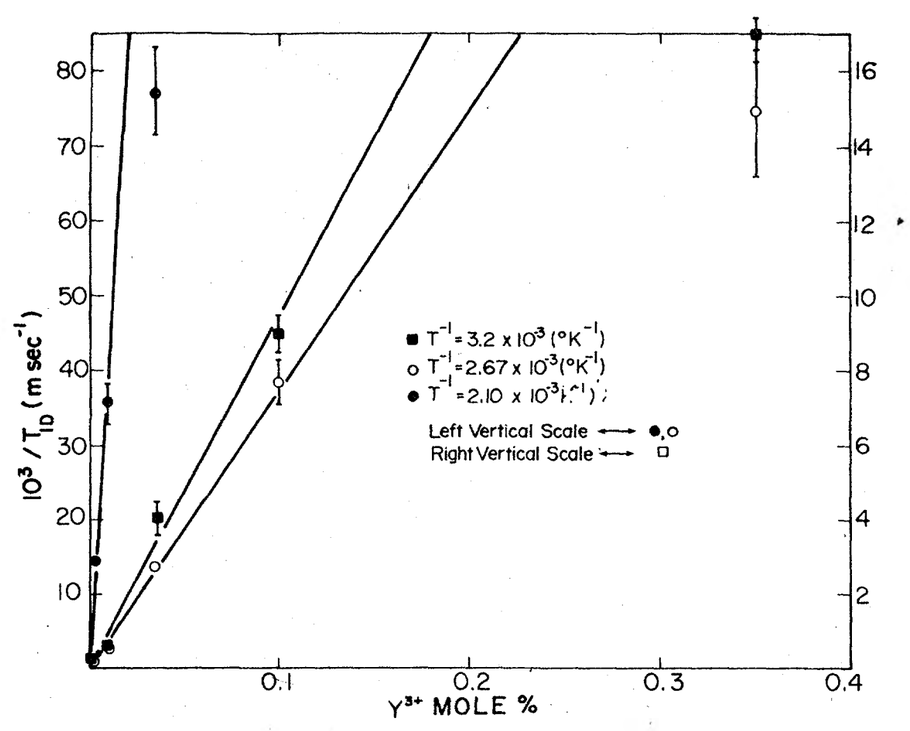

FIG. 6. Relaxation rate vs Y^{3+} dopant concentration in SrF_2 at three different temperatures.

distance in SrF_2 may result in the Y^{3+}–nn $F^-_{(i)}$ pairs being further apart from each other.

2. *Region II*

Due to the analogy between the data of $SrF_2:Y^{3+}$ and that of $CaF_2:Y^{3+}$, this region [$(3.0–2.3)\times10^{-3}$ K^{-1}] is believed to correspond to region II of $CaF_2:Y^{3+}$. As in $CaF_2:Y^{3+}$, regions III and II in $SrF_2:Y^{3+}$ also represent two different local phases. The nn $F^-_{(i)}$ may partially dissociate at around 54 °C (i.e., at 3.06×10^{-3} K^{-1}), and our observed relaxation could then arise, for example, either from $F^-_{(i)}$ jumps between nn and nnn or from $F^-_{(i)}$ jumps between equivalent nnn sites. Alternatively, as in $CaF_2:Y^{3+}$, this data may arise from motions near clusters. However, such a model leads to difficulties discussed earlier: why would the clusters be more stable at higher temperatures and in crystals with larger lattice parameter?

The activation energy computed from our $SrF:Y^{3+}$ data (0.1 mole%) is 0.17 ± 0.03 eV. Stott and Crawford[36] reported an ITC spectral peak in $CaF_2:Gd^{3+}$ corresponding to a 0.167-eV activation energy which is probably the same phenomenon.

The curve of the relaxation rate versus Y^{3+} concentration as shown in Fig. 6 is similar to that for region III, as is expected if the majority of the relaxation centers in this region do come from the dissociation of those in region III.

For more heavily Y^{3+} doped samples, Fig. 6 again indicates a possible clustering effect, which effectively decreases the number of unclustered defect complexes which may be responsible for the dominant relaxation in region II.

3. *Region I*

This region extends below the inverse temperature 2.3×10^{-3} K^{-1}. No measurements corresponding to T_{1D} shorter than 10 msec were taken, since the adiabatic condition for our ADRF pulse couldn't be satisfied for such short T_{1D}'s. Our region I in SrF_2 is similar to region I of CaF_2. The dominant relaxation centers are thus believed to be nonlocal free $F^-_{(i)}$. The activation energy determined from the undoped SrF_2 sample is 0.88 ± 0.01 eV, which is slightly lower than that for CaF_2.

Between regions I and II, the relaxation rate has contributions from both regions, as described earlier. In order to explain the data in this intermediate region, we extrapolated the region-II and region-I data for $SrF_2:Y^{3+}$ (0.01 mole%) and added the relaxation contributions. We found that the resulting relaxation curve coincides exactly with our data, as shown in Fig. 7, thus clearly demonstrating that the bending over arises merely from the sum of the mechanisms of regions I and II.

C. $BaF_2:Y^{3+}$

BaF_2 has the largest lattice constant of our three alkaline-earth fluorides and its data is also the simplest of the three as shown in Fig. 8. The curves of both the doped and undoped samples have the same shape and exhibit only two distinct regions in the whole measured temperature range. These correspond to regions I and II, respectively, in $CaF_2:Y^{3+}$ and $SrF_2:Y^{3+}$. Thus we observed no relaxation due to nn $F^-_{(i)}$, in agreement with the findings of spectroscopic measurements[19,65,68–70] which observed only trigonal and no tetragonal spectra in doped BaF_2. In region II (between 3.4×10^{-3} and 2.5×10^{-3} K^{-1}), the relaxation rate is exactly proportional to the Y^{3+} concentration up to 0.1 mole%, our maximum dopant concentration in BaF_2 (see Fig. 9). The clustering effect in BaF_2 appears to be the smallest of the three alkaline-earth fluorides as would be expected from the fact that BaF_2 has the largest lattice parameter. Our measured activation energy is 0.10 ± 0.03 eV in region II.

Above 2.5×10^{-3} K^{-1}, the relaxation is dominated by nonlocal free $F^-_{(i)}$ motion with an activation energy, 0.82 ± 0.03 eV, which is lower than that in both SrF_2 and CaF_2.

Similar relaxation time behavior in BaF_2 has been observed by Figueroa *et al.*[71]

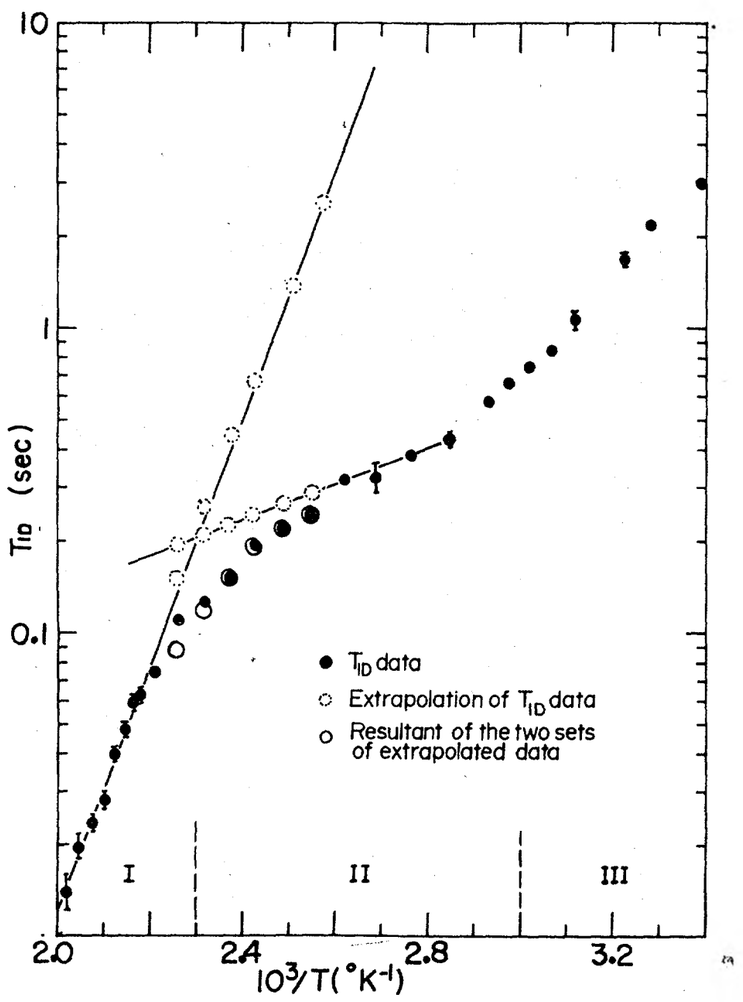

FIG. 7. Sum of relaxation rates from extensions of regions I and II in SrF_2:0.01 mole% Y^{3+}. The straight lines are extrapolations from T_{1D} data obtained from regions I and II. The hollow circles represent the resultant of these two sets of extrapolated data.

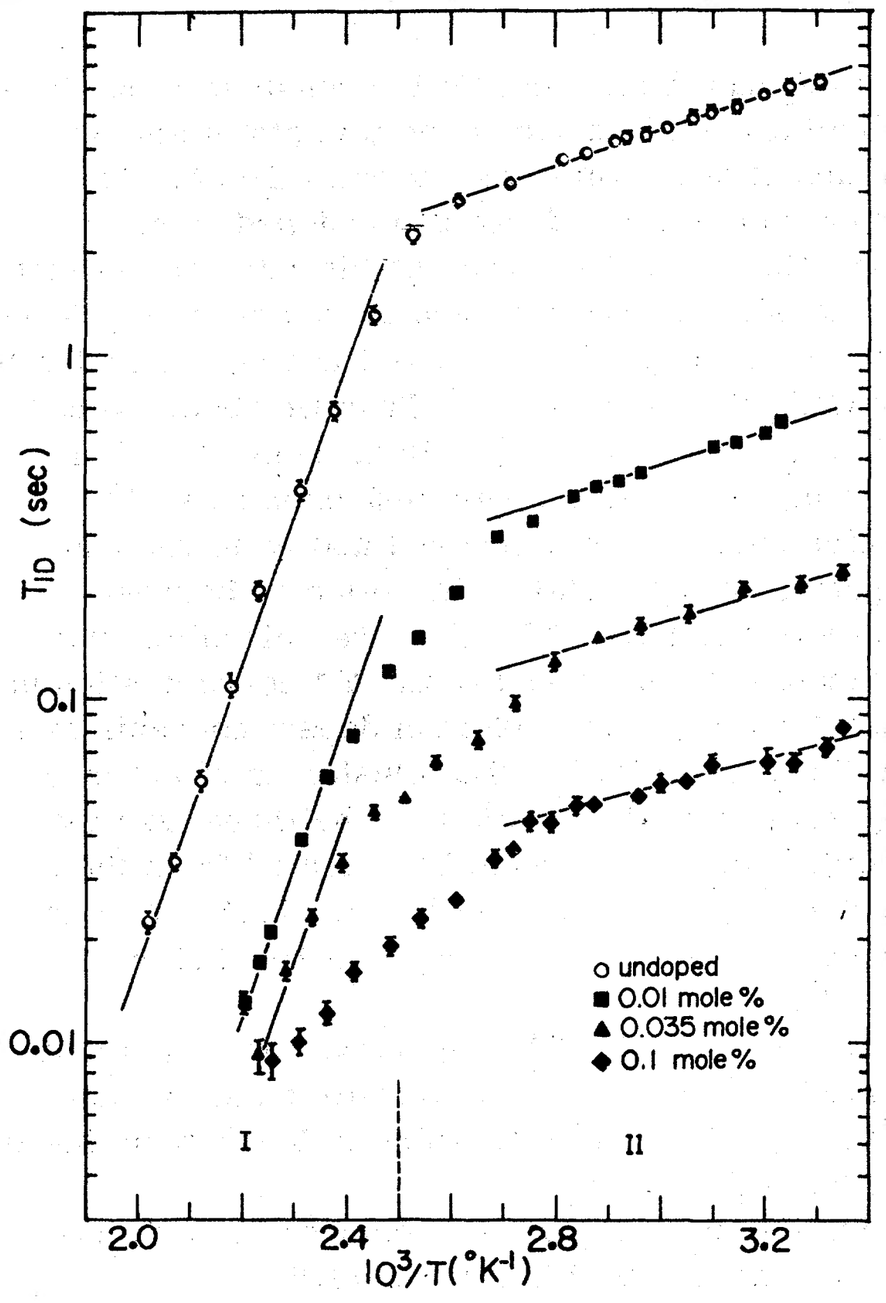

FIG. 8. Relaxation time vs reciprocal temperature in BaF_2 doped with different Y^{3+} concentrations. Solid lines are least-square fits to data.

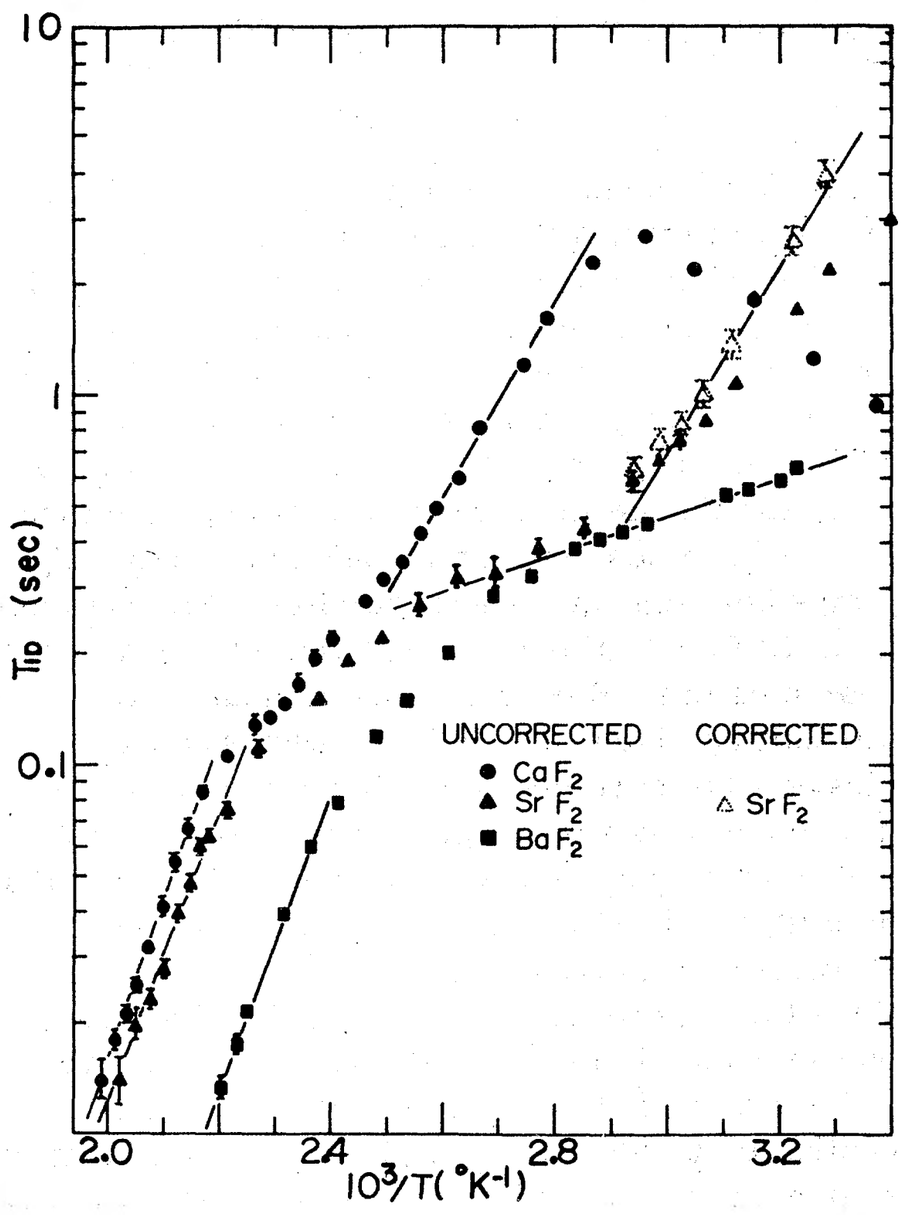

FIG. 10. Comparison of relaxation curves of CaF_2, SrF_2, and BaF_2 doped with 0.01 mole % Y^{3+}. Solid curves are least-square fits. The low-temperature line in BaF_2 is a fit only to the BaF_2 data, not to the intermediate region SrF_2 data.

D. Comparison of CaF_2:Y^{3+}, SrF_2:Y^{3+}, and BaF_2:Y^{3+} data

The best samples for comparison are the ones with medium Y^{3+} dopant concentration since they exhibit clearly all the different regions and appear to show negligible clustering effects. For this reason, we chose the 0.01-mole % Y^{3+} doped samples for our comparison. The comparison of the data of all three crystals is shown in Fig. 10.

All three crystals show a relaxation region due to nonlocal free $F^-_{(i)}$ motion. The activation energy slightly decreases in going from CaF_2 to BaF_2. Note that the transition between the nn region (e.g., region III of CaF_2 and SrF_2) and the low-activation-energy region (region II of CaF_2 and SrF_2) shifts to lower temperatures as we go from CaF_2 to BaF_2. Such behavior suggests that $F^-_{(i)}$ in the nn site of Y^{3+} becomes less stable with increasing crystal lattice parameter. (Actually, the tetragonal spectral line of R^{3+} in BaF_2:R^{3+} is barely visible in spectroscopy measurements.) In CaF_2 there are four different regions. Region IV exists in all doped and undoped samples of CaF_2, while region II is just barely visible in CaF_2:Y^{3+} (0.1 mole %). On the other hand, in BaF_2 the situation is opposite; the region IV of CaF_2 is totally absent here while the region II of CaF_2 appears strongly in all undoped and doped BaF_2 samples. SrF_2, with intermediate lattice parameter, exhibits both types of behavior over wide temperature ranges. Specifically, region III of SrF_2 has a similar slope to that of region III of CaF_2 whereas

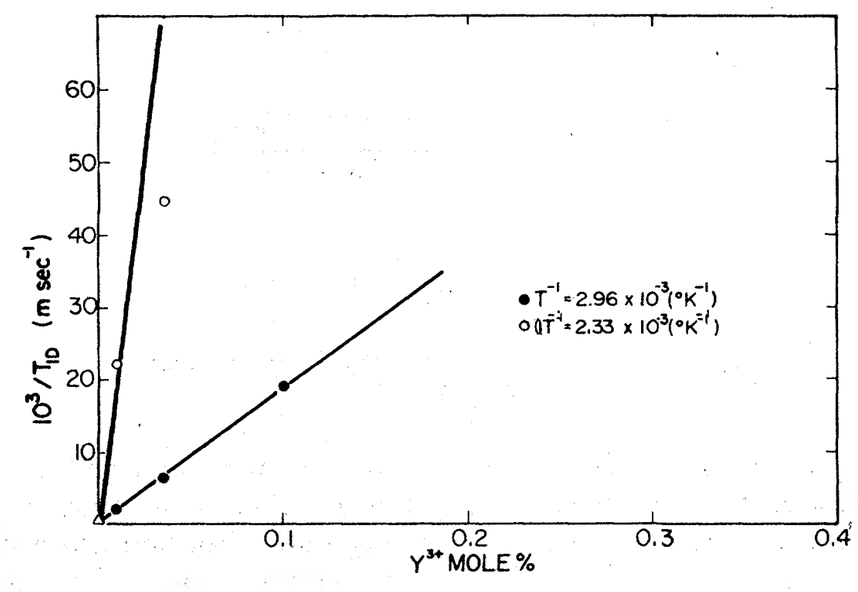

FIG. 9. Relaxation rate vs Y^{3+} dopant concentration in BaF_2 at two different temperatures.

the slope from region II of SrF_2 corresponds to that of region II of BaF_2.

This observation provides us with important insight into the relaxation mechanism of region III and II of SrF_2. As we noted earlier, spectroscopic measurements (i.e., EPR, ENDOR, and optical methods) indicate that the BaF_2 spectra at low temperatures is dominated by defects of trigonal and not tetragonal symmetry. An identification of region II of SrF_2 with this region of BaF_2 suggests that the motion of trigonal defects causes our observed NMR relaxation in SrF_2 in this region. Similarly, spectroscopic data indicating the dominance of tetragonal defects in trivalent doped CaF_2 suggests that the relaxation behavior of region III of SrF_2 is due to tetragonal (i.e., nn) $F^-_{(i)}$ defects.

E. Undoped CaF_2, SrF_2, and BaF_2

Figure 11 shows a comparison of our T_{1D} measurements in all our undoped samples. As we can see, the relaxation behavior indicates the presence in all our samples of residual charged impurities which give rise to mobile F^- ions (either F^- vacancies or F^- interstitials) for charge compensation. Normally, it is harder to identify sources of relaxation of these undoped samples in the extrinsic temperature region since the identities of these residual impurities are unknown. A discussion of the lower-temperature behavior of all samples, doped and undoped, has been presented earlier and will not be repeated in detail here. A comparison of the behavior of the two CaF_2 crystals (Optovac and Harshaw) at low and intermediate temperatures reveals that the slopes are the same, but the T_{1D}'s are different. The similarity in slopes suggests that the residual impurity arises in each crystal from the same or similar atomic species, since we have observed[9] that dopants of different size may give rise to very different slopes in this region. Furthermore, the differences in T_{1D} suggest that the impurity concentrations are different in the two samples, as we see in Fig. 11. However, it is difficult to explain the coming together of the data in the high-temperature, nonlocal region without postulating the existence in both crystals of the same concentration of a second impurity, which favors nonlocal F^- defects, as we discussed earlier.

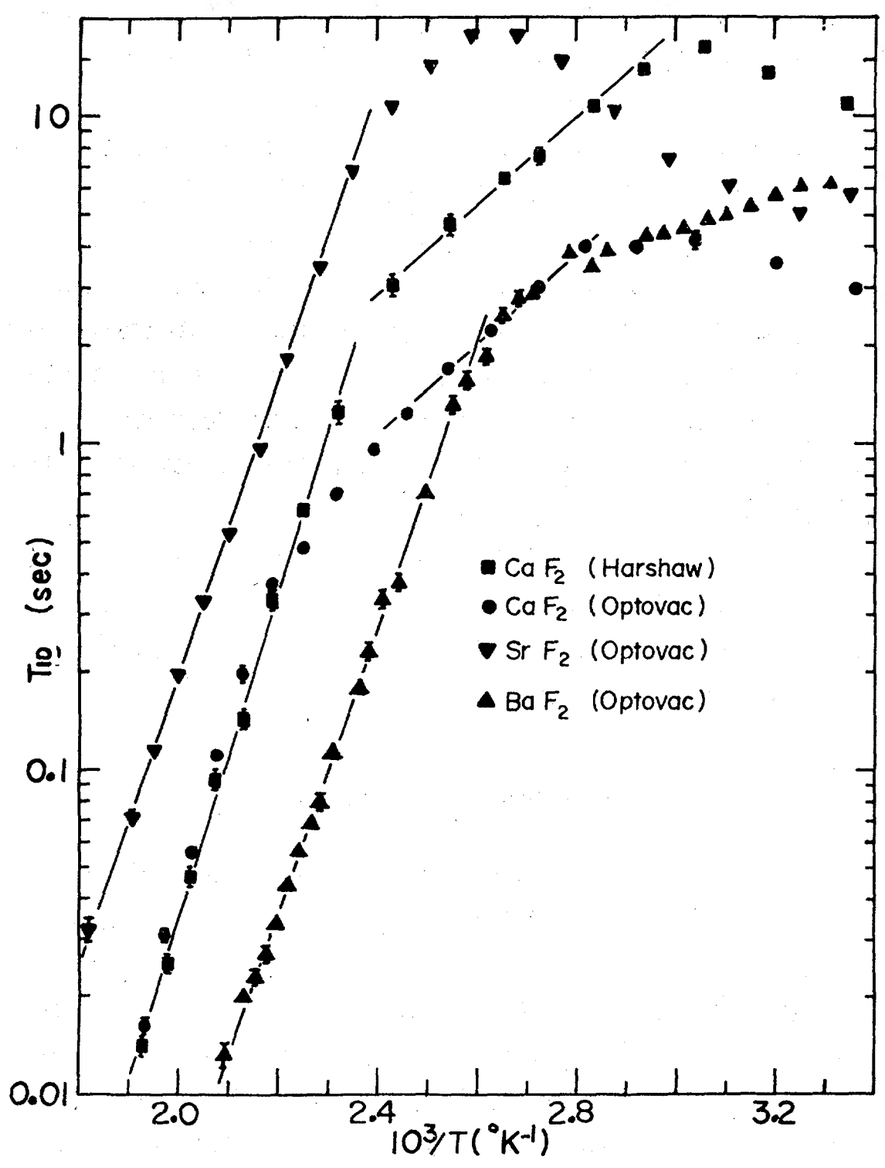

FIG. 11. Comparison of relaxation curves of undoped samples.

A possible candidate for the high-temperature relaxation in our undoped crystals could arise from the motion of fluorine vacancies created to charge-compensate residual monovalent impurities which substitute for Ca^{2+} cations. Both experimental evidence[2,53] and theoretical calculations[50-52] show that fluorine vacancies have a lower energy of motion than fluorine interstitials. Therefore, if both monovalent and trivalent impurities exist in comparable numbers in the undoped samples, one might think that fluorine vacancies would dominate the relaxation. However, our data rule out this possibility in several ways. First, the slope (or activation energy) of the undoped samples is identical with that of our Y^{3+} doped samples in which we know the mechanism to be $F^-_{(i)}$ ions. Furthermore, the slope agrees with those obtained by other workers, as shown in Table II. Second, if our relaxation in the high-temperature region were due to fluorine vacancy diffusion, the relaxation rate at a given temperature of the slightly doped Y^{3+} sample should decrease instead of increase, since, according to the mass action law, the fluorine vacancy concentration should decrease as a result of doping the sample with Y^{3+}. (Such a decrease in vacancy concentration has been verified by ionic conductivity experiments[72,73] in the intrinsic temperature region dominated by $F^-_{(v)}$ vacancy diffusion. In these experiments the intrinsic ionic conductivity of CaF_2 is observed to decrease as a result of increasing the trivalent-impurity dopant concentration.)

Furthermore, it is claimed that monovalent impurities (e.g., Na^+, K^+) are largely rejected[5] in the fluorites during crystal growth. On the other

hand, O^{2-} can easily enter the crystal[24,74] and create $F^-_{(v)}$; however, as a result of being grown in a vacuum and exposed to PbF_2, an oxygen scavenger,[74] our finished crystals are effectively free of oxygen contamination. Accordingly, we believe that the relaxation of ^{19}F spin dipolar energy is due mainly to F^- interstitials both in the low-temperature (bound $F^-_{(i)}$) and in the high-temperature (free nonlocal $F^-_{(i)}$) regions.

IV. CONCLUSION

In these experiments, we have observed ^{19}F dipolar relaxation due to jumps of both free and bound extrinsic $F^-_{(i)}$ between room temperature and 250 °C in single crystals of CaF_2, SrF_2, and BaF_2, doped with trivalent impurities.

In all three undoped alkaline earth fluorides, the high-temperature dipolar relaxation depends strongly on reciprocal temperature and indicates the existence of substantial numbers of mobile free $F^-_{(i)}$, which are probably induced by residual trivalent impurities. In this region the NMR relaxation of the bulk fluorines is due to a direct process, the "strong-collision" jumping of the abundant fluorine nuclei, probably by an interstitialcy mechanism. Since the relaxation in this region is dominated by the jumps of fluorines which are far from the dopant atoms, we would expect the relaxation times and, accordingly, the activation energies in this region to be essentially independent of the impurity dopant size, as we have observed.[9]

In the temperature regions dominated by the motions of fluorine ions bound to the dopants (regions II and III for CaF_2 and SrF_2 and region II for BaF_2), the NMR relaxation of the bulk fluorines is undoubtedly due to an indirect process in which the bulk fluorines are relaxed, not by their own diffusion jumps, but rather by the jumps of the bound fluorines which may be many lattice distances away. The heating effect due to bound fluorines then gets transmitted to the bulk fluorines by a process of spin diffusion which may be very rapid[75] for spin-$\frac{1}{2}$ nuclei like the fluorines.

We found that the relaxation due to locally bound $F^-_{(i)}$ depends very strongly on both the crystal lattice constant and the impurity dopant size.[9] In particular, the nearest neighbor bound $F^-_{(i)}$, which dominate the ^{19}F dipolar energy relaxation in the low-temperature part of our study, become increasingly unstable in the crystal having larger lattice constants, SrF_2 and BaF_2. We observed a striking decrease in slope in CaF_2 and SrF_2 data as we raised the temperature above room temperature. Such a decrease in slope cannot be explained simply by adding relaxation rates, but implies a sudden change in structure or in mechanism, as in a phase transition. We conjectured and presented evidence that this anomalous behavior may result from a partial dissociation of the complex consisting of a nn $F^-_{(i)}$ and a trivalent impurity, in which the nn $F^-_{(i)}$ moves to a more remote but still bound position (possibly a nnn). This transition occurred at around 150 °C in CaF_2:Y^{3+}, at about 54 °C in SrF_2:Y^{3+}, and presumably would occur at an even lower temperature in BaF_2:Y^{3+}. The fact that the relaxation mechanism in the intermediate region becomes more pronounced for the crystal with larger lattice distance would imply that the local lattice distortion around the dopant causes the potential wells of, say, nnn $F^-_{(i)}$ to become deeper relative to those of nn $F^-_{(i)}$ in the samples of larger lattice parameter. This behavior indicates either a different dominant local $F^-_{(i)}$ jumping mechanism or a very different energy barrier for the same type of local $F^-_{(i)}$ motion. We discussed the possibility that this low activation energy may be due to $F^-_{(i)}$ ion motion near clusters of impurities. However, this possibility appears less likely, since it implies a higher stability for such complexes at higher temperatures than at lower.

Clustering between nearby impurity–$F^-_{(i)}$ dipolar complexes is also exhibited in the dependence of our relaxation time on impurity concentration. This clustering effect decreases as we go from CaF_2 to BaF_2 and appears only in our more heavily doped samples.

The dominant relaxation mechanism in the lowest-temperature region (i.e., region IV) of CaF_2:Y^{3+} is not understood at present. The fact that the relaxation rate in this region increases with increasing Y^{3+} dopant concentration indicates that the relaxation may be due either to a different kind of local $F^-_{(i)}$ motion or to paramagnetic impurities introduced into the crystal along with the YF_3 dopant.

To the best of our knowledge, this study is the first comprehensive investigation of diffusion of both locally bound and free interstitials in the fluorites using a single technique.

ACKNOWLEDGMENTS

This work was supported by the NSF under Grant No. DMR 76-18966. We wish to thank W. A. Hargreaves of Optovac, Inc. for providing us with all samples used in this paper and for giving us details concerning the crystal growth and doping processes. Particular thanks go to Dr. D. Alderman, J. Anderson, Dr. R. Brandt, T. Case, Dr. A. R. Clayton, Dr. P. P. Ho, Dr. D. Paquette, and Dr. H. Stokes for helping us with the NMR

apparatus and computer interface. Useful discussions about the nature of the diffusion were held with Professor A. Abragam, Dr. D. Alderman, Dr. R. Briet, Dr. C. Hayes, Dr. P. P. Ho, Professor J. Jeener, Professor O. W. Johnson, Professor G. R. Miller, Professor W. D. Ohlsen, Professor C. P. Slichter, Dr. H. T. Stokes, Professor J. Strange, and Dr. D. Wolf.

---

*This paper is based on the Ph.D. thesis presented by Sherman Wei to the University of Utah (1977), unpublished.

†Present address: SEI Corp., 450 E. Ohio St., Chicago, Ill. 60611.

[1]*Nuclear Magnetic Resonance Table* by Varian Associates, 5th ed.

[2]R. W. Ure, J. Chem. Phys. 26, 1363 (1957).

[3]D. C. Ailion, Adv. Magn. Reson. 5, 177 (1977).

[4]D. C. Stockbarger, J. Opt. Soc. Am. 39, 731 (1949).

[5]W. A. Hargreaves (private communication).

[6]C. P. Slichter and W. C. Holton, Phys. Rev. 122, 1701 (1961).

[7]C. P. Slichter and D. C. Ailion, Phys. Rev. 135, A1099 (1964).

[8]P. P. Ho, Ph.D. thesis (University of Utah, 1974) (unpublished); P. P. Ho and D. C. Ailion, in *Proceedings of the 18th Ampere Congress*, edited by P. S. Allen, E. R. Andrew, and C. P. Bates (Nottingham Ampere Committee, Nottingham, 1974), Vol. 1, pp. 235–236.

[9]S. H. N. Wei, Ph.D. thesis (University of Utah, 1977) (unpublished).

[10]A. Kiel and W. B. Mims, Phys. Rev. B 6, 34 (1972).

[11]*Table of Periodic Properties of the Elements* (Sargent, Chicago).

[12]B. Bleaney, P. M. Llewellyn, and D. A. Jones, Proc. Phys. Soc. London Ser. B 69, 858 (1956); B. Bleaney, J. Appl. Phys. 33, 358 (1962).

[13]J. M. Baker, W. Hayes, and M. C. M. O'Brien, Proc. R. Soc. London Ser. A 254, 273 (1960).

[14]Yu. K. Voron'ko, G. M. Zverev, B. B. Meshkow, and A. I. Smirnov, Fiz. Tverd. Tela 6, 2799 (1964) [Sov. Phys. Solid State 6, 2225 (1965)].

[15]C. W. Rector, B. C. Pandey, and H. W. Moos, J. Chem. Phys. 45, 171 (1966).

[16]U. Ranon and J. S. Hyde, Phys. Rev. 141, 259 (1966).

[17]J. M. Baker, E. R. Davies, and J. P. Hurrell, Phys. Lett. A 26, 352 (1968); Proc. R. Soc. London Ser. A 308, 403 (1968).

[18]D. Kiro and W. Low, in *Magnetic Resonance*, edited by C. K. Coogun, N. S. Ham, S. N. Stuart, J. R. Philbrow, and G. V. H. Wilson (Plenum, New York, 1970), p. 247.

[19]J. Makovsky, in *Physics of Quantum Electronics*, edited by P. L. Kelley, B. Lax, and P. E. Tannenwald (McGraw-Hill, New York, 1966), pp. 340–349; Phys. Lett. 19, 647 (1966); Phys. Rev. Lett. 15, 953 (1965); J. Chem. Phys. 46, 390 (1967).

[20]D. R. Tallant and J. C. Wright, J. Chem. Phys. 63, 2074 (1975).

[21]J. R. O'Connor and H. A. Bostick, J. Appl. Phys. 33, 1868 (1962).

[22]M. J. Weber and R. W. Bierig, Phys. Rev. 134, A1492 (1964).

[23]Yu. K. Voron'ko, A. A. Kaminsku, and V. V. Osiko, Zh. Eksp. Teor. Fiz. 49, 420 (1965) [Sov. Phys. JETP 22, 295 (1966)].

[24]K. Muto and K. Awazu, J. Phys. Chem. Solids 29, 1269 (1968).

[25]J. B. Fenn, J. C. Wright, and F. K. Fong, J. Chem. Phys. 59, 5591 (1973).

[26]F. Z. Gil'fanov, L. D. Livanova, M. S. Orlov, and A. L. Stolov, Fiz. Tverd. Tela 11, 2203 (1969) [Sov. Phys. Solid State 11, 1779 (1970)].

[27]A. D. Franklin and S. Marzullo, Proc. Br. Ceram. Soc. 19, 135 (1971).

[28]J. L. Merz and P. S. Pershan, in *Optical Properties of Ions in Crystals*, edited by H. M. Crosswhite and H. W. Moos (Interscience, New York, 1967), pp. 117–135; Phys. Rev. 162, 217 (1967).

[29]V. B. Campos and G. F. L. Ferreira, J. Phys. Chem. Solid 35, 905 (1974).

[30]T. Rewaj, Fiz. Tverd. Tela 10, 1271 (1968) [Sov. Phys. Solid State 10, 1014 (1968)].

[31]J. H. Chen and M. S. McDonough, Bull. Am. Phys. Soc. 9, 647 (1964); Phys. Rev. 185, 453 (1969).

[32]P. D. Southgate, J. Phys. Chem. Solids 27, 1623 (1966).

[33]R. J. Lysiak and P. P. Mahendroo, J. Chem. Phys. 44, 4025 (1966).

[34]B. C. H. Royce and S. Mascarenhas, Phys. Rev. Lett. 24, 98 (1970).

[35]A. D. Franklin and S. Marzullo, J. Phys. C 3, L171 (1970); 4, 239 (1971).

[36]J. P. Stott and J. H. Crawford, Phys. Rev. B 4, 668 (1971).

[37]D. R. Stiefbold and R. A. Huggins, J. Solid State Chem. 5, 15 (1972); J. Chem. Phys. 56, 3173 (1972).

[38]J. Wagner and S. Mascarenhas, Phys. Rev. B 6, 4867 (1972).

[39]E. L. Kitts, Jr., M. Ikeya, and J. H. Crawford, Jr., Phys. Rev. B 8, 5840 (1973).

[40]E. L. Kitts, Jr., and J. H. Crawford, Jr., Phys. Rev. B 9, 5264 (1974).

[41]G. E. Matthews, Jr., and J. H. Crawford, Jr., Phys. Rev. B 15, 55 (1977).

[42]J. Fontanella and C. Andeen, J. Phys. C 9, 1055 (1976).

[43]A. D. Franklin, J. M. Crissman, and K. F. Young, J. Phys. C 8, 1244 (1975).

[44]G. D. Watkins, Phys. Rev. 113, 91 (1959).

[45]E. Friedman and W. Low, J. Chem. Phys. 33, 1275 (1960); G. Vincow and W. Low, Phys. Rev. 122, 1390 (1961).

[46]M. H. Cohen and F. Reif, in *Defects in Crystalline Solids* (The Physical Society, London, 1955), pp. 44–51; F. Reif, Phys. Rev. 100, 1597 (1955).

[47]C. Andeen, D. Link, and J. Fontanella, Phys. Rev. B 16, 3762 (1977).

[48]A. Edgar and H. K. Welsh, J. Phys. C 8, L336 (1975).

[49]C. R. A. Catlow, J. Phys. C 9, 1845 (1976).

[50]D. Chakravorty, J. Phys. Chem. Solids, 32, 1091 (1971).

[51]S. C. Keeton and W. D. Wilson, Phys. Rev. B 7, 834 (1973).

[52]C. R. A. Catlow and M. J. Norgett, J. Phys. C 6, 1325 (1973).

[53]W. Bollmann, P. Gorlich, W. Hank, and H. Mothes, Phys. Status Solidi A 2, 157 (1970).

[54]J. A. Champion, Br. J. Appl. Phys. 16, 805 (1965).

[55]J. W. Twidell, J. Phys. Chem. Solids, 31, 299 (1970).

[56]H. Matzke, J. Mater. Sci. 5, 831 (1970).

[57]F. K. Fong and M. A. Hiller, J. Phys. Chem. 71, 2854

(1967).
[58]B. R. Rossing, Ph.D. thesis (MIT, 1966) (unpublished).
[59]U. Croatts and M. Bruno, Gazz. Chim. Ital. 78, 95 (1948).
[60]J. T. Knowles and P. P. Mahendroo, Phys. Lett. A 31, 385 (1970).
[61]J. R. Miller and P. P. Mahendroo, Phys. Rev. 174, 369 (1968).
[62]E. Barsis and A. Taylor, J. Chem. Phys. 45, 1154 (1966); 48, 4357 (1968).
[63]V. V. Osiko, Fiz. Tverd Tela 7, 1294 (1965) [Sov. Phys. Solid State 7, 1047 (1965)].
[64]H. B. Johnson, G. R. Miller, and I. B. Cutler, J. Am. Ceram. Soc. 50, 526 (1967).
[65]J. Sierro, Phys. Lett. 4, 178 (1963); Helv. Phys. Acta 36, 505 (1963).
[66]M. R. Brown, K. G. Roots, J. M. Williams, W. A. Shand, C. Groter, and H. F. Kay, J. Chem. Phys. 50, 891 (1969).
[67]Y. K. Voron'ko, V. V. Osiko, and I. A. Shcherbakov, Zh. Eksp. Teor. Fiz. 55, 1598 (1968) [Sov. Phys. JETP 28, 838 (1969)].
[68]U. Ranon and A. Yaniv, Phys. Lett. 9, 17 (1964).
[69]A. A. Antipin, I. N. Kurkin, L. D. Livanova, L. Z. Potvorova, and L. Ya. Shekun, Fiz. Tverd. Tela 8, 2664 (1966) [Sov. Phys. Solid State 8, 2130 (1967)].
[70]L. A. Boatner and R. W. Reynolds, J. Chem. Phys. 52, 1248 (1970).
[71]D. R. Figueroa, A. V. Chadwick, and J. H. Strange, J. Phys. C 11, 55 (1978).
[72]V. A. Arkhangel'skaya, T. I. Nikitinskaya, and M. S. Tyutin, Fiz. Tverd. Tela 7, 2682 (1965) [Sov. Phys. Solid State 7, 2976 (1966)].
[73]T. I. Nikitinskaya, E. V. Suntsov, and M. S. Tyutin, Fiz. Tverd. Tela 9, 2111 (1967) [Sov. Phys. Solid State 9, 1656 (1968)].
[74]P. P. Fesfilov, J. Phys. Radium 17, 656 (1956).
[75]A. Abragam, *The Principles of Nuclear Magnetism* (Clarendon, Oxford, England, 1961), p. 138.